Available online at www.sciencedirect.com

SCIENCE DIRECT®

Coordination Chemistry Reviews 248 (2004) 1225–1230

COORDINATION CHEMISTRY REVIEWS

www.elsevier.com/locate/ccr

Review

Electrochemical, spectral, and quartz crystal microgravimetric assessment of conduction band edge energies for nanocrystalline zirconium dioxide/solution interfaces

Buford I. Lemon, Fang Liu, Joseph T. Hupp*

Department of Chemistry, Northwestern University, 215 Sheridan Road, Evanston, IL 60208, USA

Received 2 January 2004; accepted 17 March 2004
Available online 6 May 2004

In honor of Michael Grätzel on his 60th birthday

Contents

Abstract

Electrochemical quartz crystal microgravimetry studies of porous nanocrystalline ZrO_2 electrodes in acetonitrile containing 1 M $LiClO_4$ show that surface electronic states can be accessed at potentials as far positive as 0 V versus Ag/AgCl, as evidenced by uptake of charge-compensating cations. A much higher density of surface states is encountered beginning at about −1.3 V. Based on previous work with TiO_2, SnO_2, and ZnO, this potential is tentatively identified with E_{cb} for ZrO_2 and is about 0.5 V more negative than E_{cb} for TiO_2. In water, cation uptake is replaced by efficient reduction of H_3O^+ or water to hydrogen, a finding that has interesting parallels in radiation chemistry. Identifying the onset potential for hydrogen evolution with either E_{cb} or a potential characteristic of a high density of trap states, the value obtained is about 0.3 V negative of E_{cb} for TiO_2. Like the conduction band edge energy for titanium dioxide, the putative E_{cb} value for ZrO_2 shifts negatively with increasing pH. Comparisons of surface-based ligand-to-metal charge-transfer band energies point to an E_{cb} value for colloidal ZrO_2 in water that is about 0.4 V negative of the value for colloidal TiO_2. Consistent with three recent literature reports, empty states should lie low enough in energy to permit efficient injection from photoexcited dyes under certain conditions.

Keywords: Zirconium dioxide; Conduction band edge; Semiconductor

1. Introduction

The conduction band edge energy is a crucial parameter in the sensitization of wide bandgap semiconductors by molecular dyes in photoelectrochemical solar cells such as the titanium dioxide based Grätzel cell [1,2]. Generally the band edge must be lower in energy than the photoexcited state of the dye in order for electron injection to occur (although direct injection into lower energy surface states can sometimes be exploited to circumvent this restriction). Zirconium dioxide is often used as an unreactive surrogate or control for titanium dioxide in studies of injection dynamics, back electron transfer kinetics, and other processes [3–5]. The dye attachment chemistry of ZrO_2 is similar to that of TiO_2 and, like TiO_2, it can readily be prepared in nanocrystalline colloidal or high-area film form. Importantly, however, the band energetics of the two oxides differ

---

* Corresponding author. Tel.: +1-8474-913504; fax: +1-8474-917713.
E-mail address: j-hupp@northwestern.edu (J.T. Hupp).

0010-8545/$ – see front matter © 2004 Elsevier B.V. All rights reserved.
doi:10.1016/j.ccr.2004.03.004

significantly. Bulk zirconium dioxide is characterized by a roughly 5 eV bandgap (versus 3.2 eV for the anatase form of titanium dioxide) and a conduction band edge that is reportedly 1–1.5 V more negative (i.e. higher in energy) than that of anatase [6–8]. To our knowledge, however, there are no reports on the conduction band edge energy, E_{cb}, of nanocrystalline ZrO_2. Described below are experiments designed to evaluate E_{cb} for nanocrystalline thin films of ZrO_2 in water and in acetonitrile, and to estimate energies of probable near-band-edge surface states for aqueous colloidal suspensions of nanocrystalline ZrO_2 particles. We find that the band edge and/or surface state energies indeed are substantially more negative than those for titanium dioxide, but less so than would have been expected based on existing reports for bulk ZrO_2.

2. Experimental

Twenty weight percent colloidal suspensions of 5–10 nm diameter ZrO_2 particles in water with acetic acid as a stabilizing agent were purchased from Alfa-Aesar. The crystallinity of the particles was confirmed by X-ray powder diffraction measurements on samples from which solvent had been removed. While the suspensions were useful for catechol complexation experiments described below, they proved unsatisfactory for thin film fabrication. Sintering yielded brown, flaked films having poor mechanical stability. Consequently, colloidal samples were also prepared by the method of Xu and Anderson [9]. Briefly, 44 ml of 70% zirconium(IV)tetrapropoxide in ethanol (Aldrich) were added over several minutes, with stirring, to 600 ml of water that had been acidified by addition of 12 ml of HNO_3. A fluffy white precipitate formed immediately. After peptization for 1–3 days, a clear, stable suspension was obtained. High-area thin films were prepared by first concentrating the sols by rotary evaporation from ca. 20 to 200 to 300 $g\,L^{-1}$. Surfactant (Triton X-100) was added (1 drop mL^{-1}) and the mixture was via spin coating of the central gold-covered portion of masked quartz crystals (5 MHz, ICM). Films were then heated at 450 °C for 1.5 h. For nonaqueous experiments, the films were stored in a drying oven until just prior to use; they were then cooled in a dessicator. X-ray powder measurements indicated that the nanoparticles were amorphous prior to sintering, but crystalline afterward.

For aqueous experiments, electrolyte solutions were prepared at various pH's by adding 0.1 M $LiClO_4$ to the appropriate acid or buffer (pH 1: HCl/KCl; pH 3: potassium hydrogenphthalate/HCl; pH 7: $NaOH/KH_2PO_4$; pH 10: $KBO_3/K_2CO_3/KOH$). Solutions at $H_0 = -0.85$ were prepared as 20 wt.% H_2SO_4 with no additional electrolyte. For nonaqueous experiments, solutions were prepared from dried $LiClO_4$ and acetonitrile that had been freshly distilled from calcium hydride.

Electrochemical quartz crystal microgravimetry measurements were made with a previously described apparatus [10]. The working electrode was the ZrO_2/Au quartz-crystal assembly. A platinum wire was used as the counter electrode. Either a leak-proof Ag/AgCl electrode (Cypress Systems, E009) or an HCl-treated silver wire was used as a reference or pseudo-reference electrode. All potentials are reported versus Ag/AgCl.

3. Results and discussion

3.1. Thin-film electrodes: acetonitrile

A number of approaches exist for evaluating band edge energies (E_{cb}) for porous, high surface area semiconductor electrodes. Two that have proven useful in our lab are potential dependent near-infrared reflectance measurements and electrochemical quartz crystal microgravimetry (EQCM) [10,11]. The first has been used successfully with TiO_2 and relies upon the fact that electrons in near-band-edge surface states (traps) absorb strongly in the near-infrared region and therefore attenuate the reflectance of near-IR light. Unfortunately, the reflectance approach failed here. Apparently the near-IR extinction coefficient of the electron within ZrO_2 is too small to engender detectable reflectance attenuation. Similar difficulties have been noted previously for nanocrystalline ZnO and SnO_2 electrodes [10].

The second approach exploits the fact that electron uptake by metal-oxide semiconductors is strongly coupled to uptake of charge-compensating cations [10–16]. Indeed, advantage of the coupling has been taken by Prof. Grätzel and co-workers to construct Li^+ rocking-chair batteries featuring anatase electrodes [17]. The significance of the coupling here is that the mass of the electrode will increase once the applied potential moves negative of the conduction band edge and electrons are added. Electrode mass increases are detected as decreases in oscillation frequency (f) of the underlying quartz crystal [18]. Under optimal conditions, absolute mass changes (Δm) of as little as 0.5 ng can be detected in this fashion. The measurement can be made quantitative by using the Saurbrey equation:

$$\Delta f = \frac{-(0.057\,\mathrm{Hz\,cm^2\,ng^{-1}})\,\Delta m}{A_e} \qquad (1)$$

where A_e (=0.205 cm^2) is the active area of the electrode (i.e. the geometric footprint, not the total internal and external surface area) [19]. In favorable cases, the EQCM measurement (absolute mass change) can be combined with a measurement of the amount of charge passed (moles of electrons taken up) to determine the atomic or molecular mass, and therefore the identity, of the charge-compensating cation.

Fig. 1a shows the voltammetric response of a zirconium oxide film electrode in 1 M $LiClO_4$ in acetonitrile. The response can be ascribed to the following reaction:

$$ZrO_2 + e^-(\mathrm{external}) + Li^+(\mathrm{solution}) \rightarrow LiZrO_2\,e^-_{cb} \qquad (2)$$

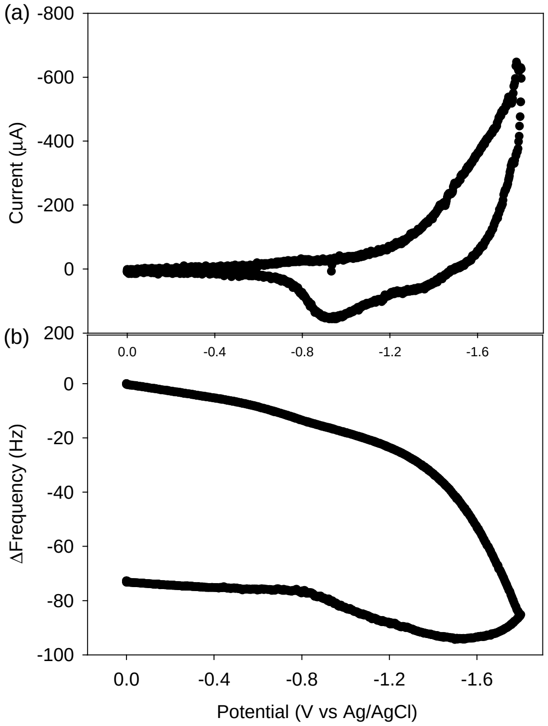

Fig. 1. (a) Current–potential curve for nanocrystalline ZrO_2 thin film immersed in 1 M $LiClO_4$/ACN solution; scan rate = 50 mV s^{-1}. (b) ΔFrequency vs. potential for the same scan, showing mass uptake upon electron addition, and partial decrease upon electron removal.

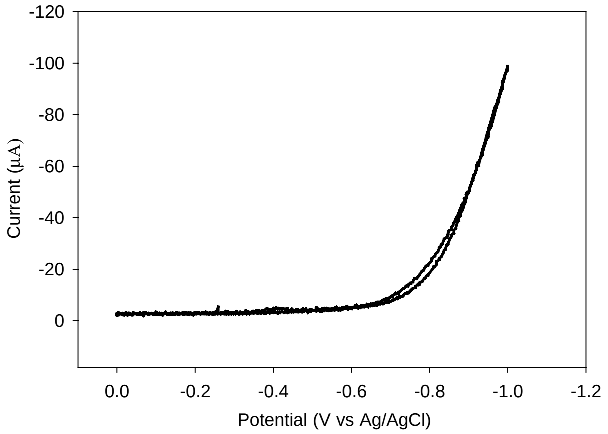

Fig. 2. Current–potential curve for nanocrystalline ZrO_2 thin film in aqueous pH 3 buffer containing 0.1 M $LiClO_4$. Scan rate = 50 mV s^{-1}.

Alternatively, a more localized (or trap based) description would be:

$$\text{Zr}^{\text{IV}}\text{O}_2 + \text{e}^-(\text{external}) + \text{Li}^+(\text{solution}) \rightarrow \text{LiZr}^{\text{III}}\text{O}_2 \qquad (3)$$

Fig. 1b shows the corresponding QCM response. As the potential is scanned in the negative direction, the electrode mass gradually increases (crystal oscillation frequency decreases) until, at about −1.3 V a sharper increase in mass is encountered. Reversal of the potential scan is initially accompanied by further mass increases, but then mass decreases. Consistent with Eqs. (2) and (3), regardless of sweep direction cathodic current flow is accompanied by mass increases and anodic current flow is accompanied by decreases. Plots of charge versus frequency change (not shown) for a number of measurements give values ranging from 5 to 18 g mol^{-1} for the charge-compensating species, suggesting Li^+ uptake but not absolutely establishing it.

The voltammetric response is characterized by what appears to be significant kinetic irreversibility. At the same time, the QCM measurements clearly point to significant chemical irreversibility; more lithium is taken up in the first part of the experiment than is released in the second part. We have encountered similar behavior with TiO_2 at low electrolyte concentrations, although better-defined behavior is seen with 1 M $LiClO_4$ [20]. Curiously, and in contrast to what is typically seen for electrochemical processes, both manifestations of irreversibility are diminished when the scan rate is increased. One interpretation is that ion uptake evolves with time from adsorption to intercalation to diffusion with deeper intercalation. By scanning more rapidly, ion release could be initiated from an adsorbed or weakly intercalated state rather than a kinetically less accessible, deeply intercalated state.

We have previously found for TiO_2, SnO_2, and ZnO that onset potentials for mass uptake agree well with independent measures of E_{cb}. The voltammetric and microgravimetric results for ZrO_2 suggest an E_{cb} value of, very roughly, −1.3 V. They also indicate the existence of accessible trap states at less negative potentials. Alternatively, the results could be interpreted to mean that a low density of traps exists in the 0 to ca. −1.3 V range, with a much higher density present at more negative potentials. For comparison, the same types of experiments for TiO_2 yield a conduction band edge energy of ca. −0.7 V versus Ag/AgCl [11]. An E_{cb} value of −1.3 V for zirconium dioxide would be insufficient to support electron injection from the lowest excited state of the well known Grätzel-cell dye, “N3” (Ru^{II}(4,4′-carboxy-2,2′-bipyridine)$(SCN)_2$) [2]. On the other hand, direct injection into trap states should be energetically feasible.

3.2. Thin-film electrodes: water

Extension of the voltammetry measurements to water as solvent yielded the peculiar result shown in Fig. 2. Only cathodic current is seen, with essentially zero hysteresis upon scan reversal. The behavior is inconsistent with the anticipated intercalation of protons and, indeed, QCM measurements show that adsorption, intercalation, and any other electrode-mass-changing processes are absent. The current flow instead is purely faradaic and can be ascribed to hydrogen evolution, either via hydronium ion or water reduction. Notably, the behavior differs from that of TiO_2, SnO_2, ZnO, and WO_3 [11,13]. These materials catalyze hydrogen formation only at potentials significantly negative of those for

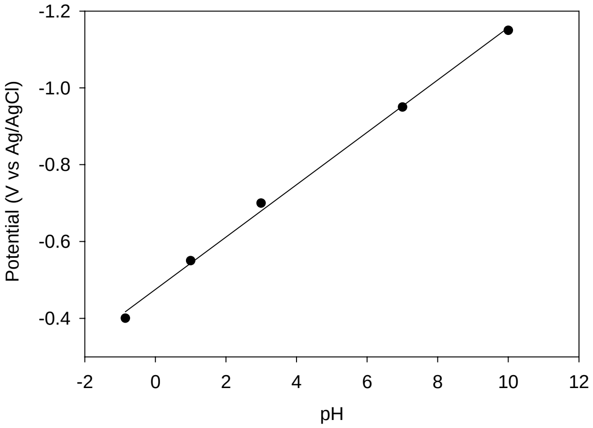

Fig. 3. pH dependence of current onset potential for ZrO_2 film in water. Linear fit to data shown, yielding slope of −68 mV/pH unit.

proton intercalation. On the other hand, the onset potential for hydrogen evolution on ZrO_2 (ca. −0.7 V at pH 3) is also well negative of the potentials where intercalation occurs for the other oxides mentioned.

An interesting and curious parallel exists in radiation chemistry. As a rule metal-oxides tend to be reasonably efficient at capturing radiolysis-generated electrons. Typically the captured electrons are largely retained in deep traps. Uniquely for zirconium dioxide, however, captured electrons are rapidly redeployed for hydrogen evolution [21]. The catalytic behavior of ZrO_2 with respect to H_2 production turns out to have important implications for an energy-conversion technology far removed from solar photoelectrochemistry: ZrO_2 is employed as a highly corrosion resistant fuel-rod and container-wall coating in nuclear pressurized-water reactors [22]. (Containers are typically constructed from zirconium alloys (zircaloy-2, 3, or 4) that spontaneously form ZrO_2 over-layers upon steam exposure [23].) While production of a potentially explosive substance such as H_2 within a reactor would clearly seem to be undesirable, the catalytic chemistry may, in fact, be beneficial. H_2 is a viable scavenger for certain highly reactive and generally undesirable, radiolytically produced species such as hydroxyl radical. Also of interest are reports of service-induced uptake of Li and H by container materials [24,25]. Lithium uptake (from aqueous solution) appears to be responsible for, or an indicator of, failure in these materials.

Returning to the electrochemical findings, if we recognize that to a first approximation an n-type semiconductor electrode material, under dark conditions, is insulating at potentials positive of E_{cb}, but conductive at potentials negative of E_{cb}, the onset potential for current flow can be viewed as a rough measure of E_{cb}. On this basis, E_{cb} is ca. −0.7 V at pH 3. As shown in Fig. 3, the onset potential shifts negatively by an average of 68 mV per unit increase in pH, in reasonable agreement with the expected shift of −59 mV per pH unit for a metal-oxide semiconductor in contact with aqueous solutions [26]. Alternatively, the onset potential at each pH could correspond to the least negative potential where a very high density of surface states exists. We recognize that the definition of “onset potential” is a bit arbitrary; we also recognize that these interpretations neglect any contributions from additional kinetic overpotential for hydrogen evolution. (On the other hand, if a significant additional kinetic overpotential existed, as in the case of TiO_2 or SnO_2, proton intercalation ought to be observed at potentials positive of the onset potential for hydrogen evolution.) Despite the ambiguity, the experiments do provide a good measure of the potential at each pH where electron transport can be sustained. For comparison, E_{cb} for titanium dioxide is less negative: ca. −0.4 V versus Ag/AgCl at pH 3.

3.3. Colloidal suspensions: water

An interesting alternative method for estimating E_{cb} is to measure interfacial charge-transfer absorption energies. Catechol, **1**, is representative of colorless compounds that form chromophoric surface complexes upon binding to certain metal-oxides [27]. Binding occurs via deprotonation of the catechol and chelation of an oxide-bound metal center. Light absorption corresponds to excitation of a ligand-to-metal charge-transfer transition. Collectively, the empty d orbitals of zirconium dioxide and titanium dioxide comprise the respective conduction bands of these materials. Nevertheless, because of the potential state-localization effects of chelation itself, the acceptor site for catechol-to-surface charge-transfer is probably better viewed as a near-band-edge trap than as the overall conduction band.

1

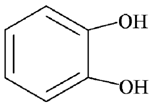

Consistent with several previous reports [27–29], we find that catechol binding to colloidal titanium dioxide produces an easily observed charge-transfer (CT) band with a peak at 410 nm (3.02 eV). As shown in Fig. 4, catechol binding to colloidal zirconium dioxide produces a charge-transfer band with a maximum at 366 nm (3.39 eV). A titration experiment in which ZrO_2 colloid is added in excess to a known amount of catechol until all of the catechol is bound, yields an extinction coefficient at 366 nm of 500 M^{-1} cm^{-1}. A related experiment (inset of Fig. 4) shows that the binding can be fit to a Langmuir isotherm with a binding constant of 4×10^3 M^{-1}. Comparing ZrO_2 to TiO_2, the difference in CT band energy is a measure of the energy difference between near-band-edge surface states for the two materials. If the pertinent surface states lie equally close in energy to the respective conduction band edges (admittedly, a speculation that is unproven), then the CT band energy difference is also a measure of the E_{cb} difference for the two materials. On this basis, the conduction band edge energy for ZrO_2 is

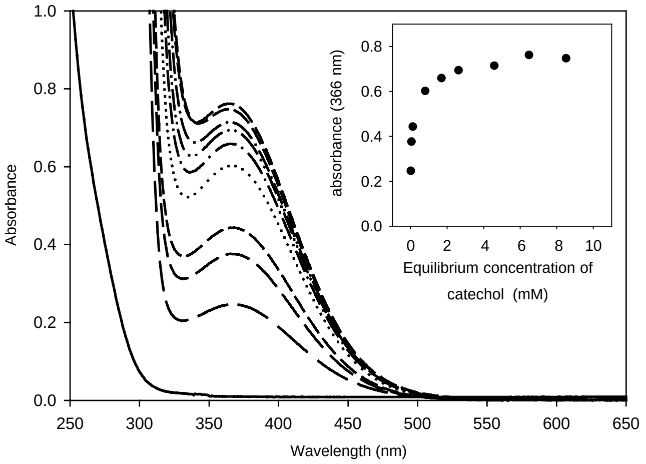

Fig. 4. UV-Vis extinction spectra of colloidal ZrO_2 in water (solid line) with progressive additions of catechol. Inset: Equilibrium concentration of catechol and absorbance at 366 nm (λ_{max}).

~ -0.85 at pH 3.7. Adjusted to pH 3, the estimated value of E_{cb} for ZrO_2 is -0.8 V versus Ag/AgCl, in good agreement with the value inferred from voltammetry experiments.

4. Conclusions

EQCM studies of porous nanocrystalline ZrO_2 electrodes in acetonitrile containing 1 M $LiClO_4$ show that surface electronic states can be accessed at potentials as far positive as 0 V versus Ag/AgCl, as evidenced by uptake of charge-compensating cations. A much higher density of surface states is encountered beginning at about -1.3 V. Based on previous work with TiO_2, SnO_2, and ZnO, this potential is tentatively identified with E_{cb} for ZrO_2 and is about 0.5 V more negative than E_{cb} for TiO_2. In water, cation uptake is replaced by efficient reduction of H_3O^+ or water to hydrogen, a finding that has interesting parallels in radiation chemistry. Identifying the onset potential for hydrogen evolution with either E_{cb} or a potential characteristic of a high density of trap states, the value obtained is about 0.3 V negative of E_{cb} for TiO_2. Like the conduction band edge energy for titanium dioxide, the putative E_{cb} value for ZrO_2 shifts negatively with increasing pH. Comparisons of surface-based ligand-to-metal CT band energies point to an E_{cb} value for colloidal ZrO_2 in water that is about 0.4 V negative of the value for colloidal E_{cb} value for colloidal TiO_2.

We conclude that under some conditions, ZrO_2 will not behave innocently and dye injection should be possible. Indeed, at least three examples of successful electron injection exist. Olsen et al. found that the standard Grätzel cell dye, Ru^{II}(4,4′-carboxy-2,2′-bipyridine)$(SCN)_2$, could inject from an upper excited state, but not from lower-energy states, in water, acetonitrile, or methanol as solvent [30]. Evidently injection from the upper state is faster than vibrational and/or electronic relaxation. Huber and co-workers found that alizarin could inject directly into surface electronic states of aqueous colloidal ZrO_2 [31]. Hao and co-workers found that coumarin-343 could inject into zirconium dioxide in acidic water as solvent, but not in heptane [29]. They ascribed the reactivity to direct injection into surface states.

Acknowledgements

We gratefully acknowledge the Basic Energy Sciences Program, Office of Science, US Department of Energy for financial support of our work (grant no. DE-FG02-87ER13808).

References

[1] B. O'Regan, M. Grätzel, Nature 353 (1991) 737.
[2] A. Hagfeldt, M. Grätzel, Acc. Chem. Res. 33 (2000) 269.
[3] A. Kay, R. Humphrey-Baker, M. Grätzel, J. Phys. Chem. 98 (1994) 952.
[4] N.J. Cherepy, G.P. Smestad, M. Grätzel, J.Z. Zhang, J. Phys. Chem. 101 (1997) 9342.
[5] Y. Tachibana, J.E. Moser, M. Grätzel, D.R. Klug, J.R. Durrant, J. Phys. Chem. 100 (1996) 20056.
[6] H.H. Kung, H.S. Jarrett, A.W. Sleight, A. Ferretti, J. Appl. Phys. 48 (1977) 2463.
[7] J.G. Bendoraitis, R.E. Salomon, J. Phys. Chem. 69 (1965) 3666.
[8] P. Clechet, J.-R. Martin, R. Olier, C. Vallouy, C. R. Acad. Sci. C 282 (1976) 887.
[9] Q. Xu, M.A. Anderson, J. Mater. Res. 6 (1991) 1073.
[10] B.I. Lemon, J.T. Hupp, J. Phys. Chem. B 101 (1997) 2426.
[11] L.A. Lyon, J.T. Hupp, J. Phys. Chem. 99 (1995) 15718.
[12] B.I. Lemon, L.A. Lyon, J.T. Hupp, in: J.H. Fendler (Ed.), Nanoparticles in Solids and Solutions. Preparation, Characterization and Applications, VCH-Wiley, Weinheim, 1998, p. 335.
[13] B.I. Lemon, J.T. Hupp, J. Phys. Chem. 100 (1996) 14578.
[14] D.B. Le, S. Passerini, A.L. Tipton, B.B. Owens, W.H. Smyrl, J. Electrochem. Soc. 142 (1995) L102.
[15] S.I. Cordoba de Torresi, A. Gorenstein, R.M. Torresi, M.V. Vazquez, J. Electroanal. Chem. 318 (1991) 131.
[16] D. Fattakhova, L. Kavan, P. Krtil, J. Solid State Electrochem. 5 (2001) 196.
[17] S.Y. Huang, L. Kavan, I. Exnar, M. Grätzel, J. Electrochem. Soc. 142 (1999) L142.
[18] D.A. Buttry, in: A.J. Bard (Ed.), Electroanalytical Chemistry, Marcel Dekker, New York, 1991 (Chapter 1).
[19] G. Sauerbrey, Z. Phys. 155 (1959) 206.
[20] B.I. Lemon, Ph.D. Thesis, Department of Chemistry, Northwestern University, 1999.
[21] J.A. LaVerne, L. Tandon, J. Phys. Chem. B 106 (2002) 380.
[22] R.A. Perkins, R.A. Busch, in: C.M. Eucken, A.M. Garde (Eds.), Zirconium in the Nuclear Industry: Ninth Annual Symposium. ASTM STP 1132, American Society for Testing and Materials, Philadelphia, 1991, p. 595.
[23] H.-J. Beie, A. Mitwalsky, F. Garzarolli, H. Ruhmann, H.-J. Sell, in: A.M. Garde (Ed.), Zirconium in the Nuclear Industry: Tenth Annual Symposium. ASTM STP 1132, American Society for Testing and Materials, Philadelphia, 1994, p. 615.
[24] N. Ramasubrumanian, in: C.M. Eucken, A.M. Garde (Eds.), Zirconium in the Nuclear Industry: Ninth Annual Symposium. ASTM STP 1132, American Society for Testing and Materials, Philadelphia, 1991, p. 613.
[25] M.B. Elmoselhi, B.D. Warr, S. McIntyre, in: A.M. Garde (Ed.), Zirconium in the Nuclear Industry: Tenth Annual Symposium. ASTM

STP 1132, American Society for Testing and Materials, Philadelphia, 1994, p. 62.
[26] J.M. Bolts, M.S. Wrighton, J. Phys. Chem. 80 (1976) 2641.
[27] J. Moser, S. Punchihewa, P.P. Infelta, M. Grätzel, Langmuir 7 (1991) 3012.
[28] Y. Liu, J.I. Dadap, D. Zimdars, K.B. Eisenthal, J. Phys. Chem. B 103 (1999) 2480.
[29] E. Hao, N.A. Anderson, J.B. Asbury, T. Lian, J. Phys. Chem. 106 (2002) 10191.
[30] C.M. Olsen, M.R. Waterland, D.F. Kelley, J. Phys. Chem. 106 (2002) 6211.
[31] R. Huber, S. Spörlein, J.E. Moser, M. Grätzel, J. Wachtveitl, J. Phys. Chem. 104 (2000) 8995.